Reignition Dynamics in Massively Parallel Direct Numerical Simulations of CO/H$_2$ Jet Flames

E.R. Hawkes[1], R. Sankaran[2], and J.H. Chen[3]

[1]School of Photovoltaic and Renewable Energy Engineering,
University of New South Wales, New South Wales, 2052, AUSTRALIA

[2]National Centre for Computational Sciences,
Oak Ridge National Laboratories, MS 6008 PO Box 2008, Oak Ridge, TN 37831-6008, USA

[3]Combustion Research Facility,
Sandia National Laboratories, MS 9051, PO BOX 969, Livermore, CA 94551-0969, USA

Abstract

Massively parallel three-dimensional DNS of turbulent temporally evolving nonpremixed plane jet flames have been performed with realistic CO/H$_2$ kinetics. Up to 0.5 billion grid points were employed allowing jet Reynolds numbers of 9000 to be attained. Simulations were run on up to 4096 processors and generated more than 30 TB of raw data. New results are presented concerning the extinction and reignition dynamics occurring in these flames. We characterise extinction using a metric based on the total stoichiometric flame surface area having a reacting scalar such as a product or radical species less than a threshold value taken to represent extinction. The motion of edge flames separating extinguished and burning regions of this surface is studied using a massively parallel analysis tool. The joint probability density function of the local edge flame speed relative to the flow and scalar dissipation has been extracted and shows a transition in character as the simulation progresses. The transition is interpreted in the context of the physical mechanisms of extinction and reignition. Along with other evidence it indicates that the mechanism of folding by turbulence of burning regions onto extinguished ones is the dominant reignition mechanism. The effect of the choice of the scalar species, scalar cut-off value, and mixture fraction value used to define extinction is discussed.

Introduction

In nonpremixed combustion, fuel-oxidiser mixing takes places simultaneously with combustion and hence the rate of combustion is closely linked to the rate of mixing. Rapid mixing is often desirable in practical combustors to increase heat release rates, enabling smaller combustor chambers. Problems may arise however when rates of mixing exceed combustion rates, leading to local extinction of flames. Following this, local regions of fuel and oxidiser can mix and coexist without significant reaction, and may later reignite. The rates of extinction and reignition are important to predict the flame stability and pollutant emissions. However, the physical mechanisms of reignition that occur in turbulent flames are not yet fully understood, nor are models of turbulent combustion yet capable of predicting them [1].

While significant advances have been made in experimental measurements of flames, the capability to simultaneously measure the temporal and three-dimensional variations of multiple reacting scalars that is necessary to understand the process of extinction and reignition does not yet exist. However, advances in computing have brought opportunities to perform direct numerical simulations (DNS) that can access such data, albeit in a limited regime of parameter space. Massively parallel DNS of turbulent nonpremixed plane jet flames have been performed with CO/H2 kinetics [2]. Up to 500 million grid points were employed, utilizing up to 4096 computer processors, and allowing jet Reynolds numbers of up to 9000 to be achieved with good resolution. The simulations feature strong finite-rate chemistry effects including extinction and reignition, and will be used to understand fundamental aspects of turbulence-chemistry interactions and to provide a numerical benchmark for the advancement of combustion models. Figure 1 shows an image of scalar dissipation rate from the simulations, generated using hardware-accelerated parallel volume rendering software [3,4]. The wide range of scales that is visually evident shows that a fully turbulent flow has been achieved.
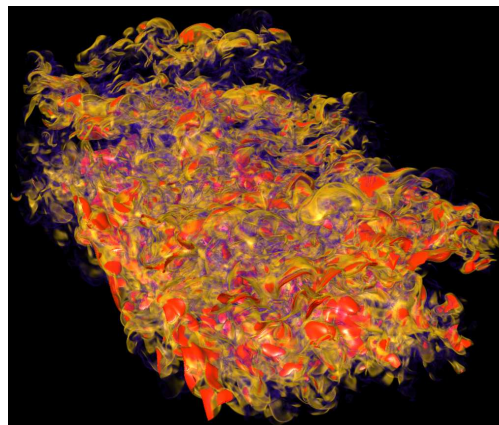

Figure 1: Volume rendering of scalar dissipation rate in a DNS of a temporally evolving jet flame

In this paper we present an analysis of the extinction-reignition phenomena that are observed in the DNS. Extinction is characterized using a measure based on the total area of an iso-mixture fraction surface having a reacting scalar such as a product or radical species greater than a threshold value taken to represent extinction. The evolution of this measure is linked to the motion of "edge flames" separating the regions having a scalar value above or below the threshold. The edge flame motion is analysed to show that reignition occurs primarily by turbulence folding burning flame sections onto non-burning ones.

Evolution of Burning Flame Area

Due to the large quantity of the DNS data (more than 30 Terabytes) and the complexity of the physical phenomena of extinction and reignition in a multiple species reacting flow, some simplifications must be made in order to provide clear physical interpretations. Our first simplification is to study only

the evolution of the area of a surface having a single mixture fraction value rather than the entire flame. This choice is made because it is known that in many conditions of practical interest, reaction is confined to thin sheets close to the stoichiometric mixture fraction [5]. Our second simplification is that we consider areas of this surface to be either "burning" or "extinguished", depending on whether the value of a reacting scalar (such as a product, radical species or temperature) is above or below a threshold. This simplification is expected to be most appropriate for high activation energy flames, which result in strongly bi-modal conditional probability density functions (pdfs) of reacting scalars [6,7].

We define the conditional surface density as:

$$\Sigma_{\varphi>\varphi^*} = \overline{|\nabla Z| \delta(Z - Z^*) H(\varphi - \varphi^*)} \quad (1)$$

Where Z is Bilger's mixture fraction, Z^* is the particular value of Z being considered, φ is a reacting scalar defined on the surface, φ^* is the threshold value of this scalar below which the flame is considered extinguished, δ is the Dirac function, and H is the Heaviside function. The overbar represents an averaging operation, either a conventional Reynolds average or a spatial filtering as in Large Eddy Simulation. Here, for simplicity, we use a Reynolds average and ignore any transverse dependence. The result is a single time-varying quantity $A_{\varphi>\varphi^*}$, representing the total amount of "burning flame surface area" in the domain. The evolution equation of this conditional surface area has been derived [8] and is similar to the evolution equation of the unconditional surface area (appearing in traditional coherent flame modelling [9,10]), the primary difference being that it contains an additional term corresponding to the propagation of the intersection line of the stoichiometric and scalar threshold isosurfaces. Under our assumptions, this term is linked with the motion of edge flames separating extinguished and burning regions. We find that the speed of these edges, denoted s_{edge}, is given by:

$$s_{edge} = \frac{s_\varphi - k s_z}{\sqrt{1 - k^2}}, \quad (2)$$

where s_φ is the displacement speed of the scalar isosurface, given by $s_\varphi = \frac{D\phi}{Dt}/|\nabla \phi|$, s_z is the displacement speed of the mixture fraction isosurface, given by $s_z = \frac{DZ}{Dt}/|\nabla Z|$, and k is the inner product of the normal vectors to these isosurfaces. Note that this expression may be shown to be equivalent to that used by Pantano [11], although an explicit expression was not given there, and a link was not made with the conditional surface area.

A massively parallel analysis tool has been developed to extract flame edges. The algorithm uses a ghost zones strategy combined with marching cubes to first extract a set of triangles representing the iso-mixture fraction surface. The triangle edges are then searched to find intersections with the scalar isosurfaces. All quantities required at the flame edges are evaluated as three-dimensional field quantities using the same high-order differencing stencil as employed in the simulation code [12], and are then interpolated to the flame edge positions, employing a ghost zones strategy for the parallelism. Statistics are then collected from these data in a serial post-processing step.

The stoichiometric value is selected to define the mixture fraction isosurface. The hydroxyl radical (OH) mass fraction is selected as the scalar to mark extinction. This choice was made after a visual inspection of the fields of heat release and OH showed a good correspondence during periods of maximum extinction. We select the cut-off value of Y_{OH} equal to 0.0007, which is half of the value at the steady extinction condition, and results in a total extinguished flame surface area that is approximately half of the total stoichiometric surface area at the time of maximum extinction. The sensitivity of our results to all of these choices is under study and will be presented in the final version of this work. To increase the level of statistical convergence, results presented on this paper have been averaged over several data-snapshots centered on a particular simulation time. The averaging window corresponds to $2t_j$, where t_j is the characteristic jet timescale and approximately $45t_j$ are simulated. Experimentation with the size of the averaging window shows that it does not affect the qualitative results – the quantities shown here vary over timescales larger than $2t_j$. Here, results are shown only for Case M of Hawkes et al. [2], with a jet Reynolds number of approximately 4500. Analysis for the other simulated cases is in progress.

Results

Figure 1 shows an example of the stoichiometric isosurfaces at two different times. The left images show the surface coloured by the scalar dissipation rate, $\chi = 2D|\nabla Z|^2$ [13], where D is the diffusivity of the mixture fraction assuming unit Lewis numbers. Higher χ regions are shown in white, through red for intermediate values and the lowest values are in black. The right images show the surface coloured in black where $\varphi < \varphi^*$ and in gold where $\varphi > \varphi^*$. The view is in the transverse (homogeneous) direction from the oxidizer side. The boundary conditions in the streamwise (left-right) and spanwise (top-bottom) directions are periodic. The mean flow is to the left closer to the viewer and to the right towards the middle of the fuel jet (which is obscured by the surface). The upper images corresponds to an early time during the simulation ($10t_j$), when the first extinguished regions are appearing, and the lower images corresponds to a later time ($20t_j$), near the time of maximum extinction. The first extinguished areas are observed on structures that bulge out towards the oxidizer side. These areas also correspond to regions of high χ. At later times, the extinguished regions are more prevalent and there is no clear correspondence with any particular structure or scalar dissipation.
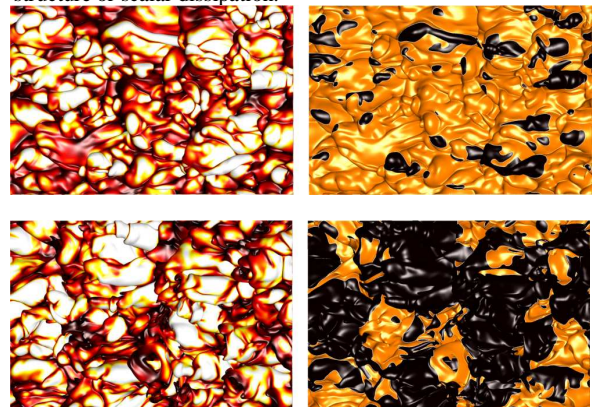
Figure 1: Stoichiometric mixture fraction surface coloured by scalar dissipation on the left and in black where $\varphi < \varphi^*$ and in gold where $\varphi > \varphi^*$ on the right.

Figure 2a (left) shows the mean extinguished flame area versus time, given by $A_{\varphi<\varphi^*} = A - A_{\varphi>\varphi^*}$, where A is the total stoichiometric surface area. The extinguished area first increases, corresponding to increasing local extinction, and then

decreases, corresponding to reignition. The mean flame edge speed is shown versus time in Figure 2b (right). This speed is normalized by the theoretical speed of a laminar propagating triple flame $s_{ref} = \sqrt{\dfrac{\rho_u}{\rho_b}} s_L$ [14], where s_L is the laminar flame speed and ρ_u are the ρ_b unburned and burned mixture densities respectively. Initially the speed is strongly negative, which by our definition corresponds to opening extinction holes, then later becomes positive to achieve reignition by closing the extinction holes. Note that during the reignition phase, the mean speed is larger than the theoretical laminar propagation speed.
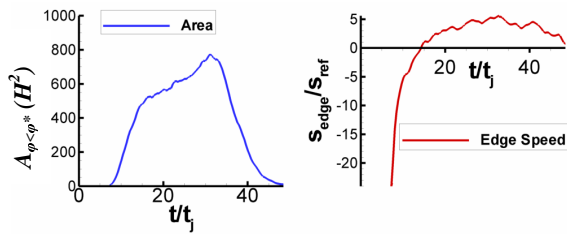

Figure 2. a) Left: normalized total extinguished flame area versus time. b) Right: normalized mean edge flame speed versus time.

A much greater level of detail is provided by extracting the joint probability density function (pdf) of the local edge flame speed and scalar dissipation. This shows a transition in character as the simulation progresses that has not been observed in previous work.. Figure 2 shows this joint probably density function for three simulation times corresponding to (from left to right) strong extinction ($10t_j$), a transitional state ($20t_j$), and strong re-ignition ($30t_j$). The color scale shows the joint pdf while the mean speed conditional on χ is shown in a black line. Scalar dissipation (χ) is normalized by the steady extinction value (χ_q) while the edge speed (s_{edge}) is again normalized by s_{ref}. At the early time, a strong negative correlation is observed, and the general shape of the pdf is in agreement with earlier work by Pantano [11] in simulations of the near field of a spatially developing jet flame, and previous asymptotic results for laminar flames [15]. Later, two branches develop with a positive correlation occurring at low and intermediate scalar dissipation. At the latest time, there is a noticeable peak in the conditional mean speed – the maximum reignition rate clearly occurs at quite a high value of χ. Previous simulations of a spatially developing jet flame were limited to the near field and were unable to capture this temporal development [11]. We attribute the existence of this positive correlation at low and intermediate χ to reignition events occurring by turbulence folding burning flame sections onto non-burning ones [16].
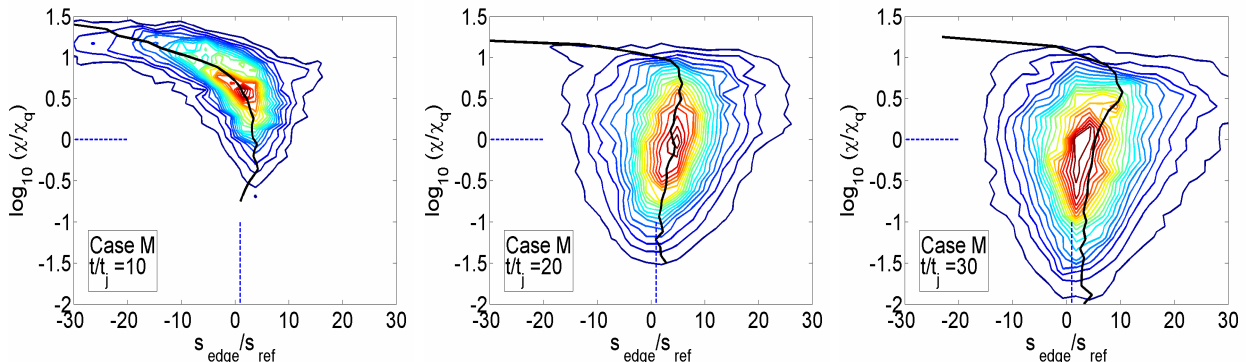
Locally, this requires that stoichiometric surfaces must be brought into close contact, leading to locally high χ at these reignition sites. We will refer to this reignition scenario as "turbulent folding", and it essentially corresponds to the "perpendicular engulfment" scenario described in Sripakagorn et al. [6]. This is contrasted against a scenario in which extinguished regions reignite by the propagation of a laminar-like edge flame along the stoichiometric surface, which we will refer to as "edge flame propagation".

Evidence of our explanation is provided by examining the magnitude of inner product of the normal vectors to the scalar and mixture fraction isosurfaces, $|k|$. The mean value of this quantity over all flame edge locations, conditional on the scalar dissipation and edge speed is shown in Figure 4 on the color scale at the time $30t_j$. Isocontours of the joint pdf of scalar dissipation and edge speed are overlaid in white and the conditional mean speed is overlaid in black. It may be observed that higher values of the inner product, which correspond to the mixture-fraction and scalar isosurfaces being aligned, tend to occur at high scalar dissipation rates and high positive edge flame speeds – this is exactly the situation that is expected for reignition by "turbulent folding". Where "edge flame propagation occurs", it is expected that the reacting scalar and mixture fraction will be poorly aligned at the reignition point, since the flame is propagating approximately parallel to the mixture fraction isosurfaces. This corresponds to low values of $|k|$, which are observed here for low values of scalar dissipation, and positive but low values of the edge flame speed. Thus both modes of reignition are simultaneously present, however the much larger propagation rates in the flame folding mode imply that this mechanism is dominant. Although the results are presented in a very different way, the qualitative finding is in general agreement with that of Sripagakorn et al. [6], who found a mixed mode of reignition with edge flame propagation dominant at early times and a transition towards turbulent folding as time progresses. Here, we shed additional light on the process by examining the shear flow instead of a homogeneous flow, and linking the reignition rate directly with a definable metric for extinction related to the flame area, rather than considering an ensemble of iso-surface following particles, which tend to accumulate in areas of negative tangential stretch rate and thus skew any averaged statistics.
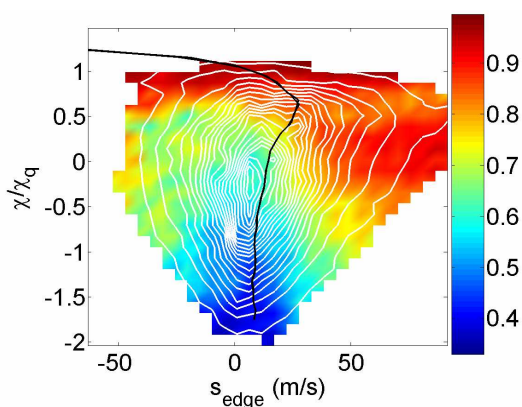

Figure 3: Joint pdf of normalized edge flame speed and scalar dissipation rate at three different simulation times.

Figure 4: Inner product of scalar and mixture fraction normals, conditionally averaged on scalar dissipation and edge flame speed.

Conclusions

Massively parallel, three-dimensional direct numerical simulations of temporally evolving turbulent CO/H_2 plane jet flames employing a skeletal chemistry model were analysed to shed light on the phenomena of extinction and reignition. A total "extinguished" iso-mixture fraction surface area, defined according to a threshold value of a reacting scalar such as a product or radical species on the surface, was introduced as a marker of the total amount of extinction. Use of this marker led naturally to the consideration of the motion of the flame-edges that separate areas above and below the threshold. Analysis of the behaviour of the joint pdf of the edge flame speed and scalar dissipation shows a transition in character that has not previously been observed. At early times, during extinction, the edge flame speed shows a strong negative correlation with scalar dissipation, as previously found, but this then transitions during reignition into a situation where the speed is positively correlated with scalar dissipation at low and intermediate scalar dissipation rates and becomes negatively correlated only at extreme dissipation rates. The result is that the peak reignition rate occurs at a moderately high dissipation rate. We use evidence of the alignment of the normals to the mixture-fraction and reacting scalar isosurfaces to show that these high reignition rates tend to occur where heat and radicals are being supplied normal to the flame surface, as turbulent straining brings burning and non-burning sections of the flame surface into close proximity. We also find that simultaneously reignition can occur by propagation of edge flames along the stoichiometric surface in regions of low scalar dissipation rate. However the propagation rates of these structures are significantly lower and we find the scenario of reignition by "turbulent folding" to be dominant. Work is in progress to assess the effect of our assumptions on the results – namely, the choice of mixture fraction isosurfaces, the choice of reacting scalar and its threshold value. We are also investigating the influence of Reynolds number and differential diffusion on the findings.

Acknowledgments

References

[1] International Workshop on Measurement and Computation of Turbulent Nonpremixed Flames, http://www.ca.sandia.gov/TNF/abstract.html

[2] Hawkes, E.R., Sankaran, R., Sutherland, J.C., Chen, J.H., (2007), Proc. Combust. Inst. 31:1633-1640.

[3] Ma, K.-L., Yu, H., Chen, H., Chen, J.H., Hawkes, E.R., (2005), Simultaneous visualization of simulated combustion data, Storcloud application demonstration at *Supercomputing 05 High Performance Computing, Networking and Storage Conference*, Seattle, WA, Nov. 12-18.

[4] Akiba, H., Ma, K.-L., Chen, J.H., Hawkes, E.R., (2007), Visualizing multivariate volume data from turbulent combustion simulations, IEEE Computing in Science & Engineering, Volume 9, Number 2, March/April 2007, pp. 86-93.

[5] Veynante, D., Vervisch, L., (2002), Turbulent combustion modeling, Prog. Energy and Combust. Sci. 28:193-266.

[6] Sripakagorn, P., Mitarai, S., Kosály, G., Pitsch, H., (2004), Extinction and reignition in a diffusion flame: a direct numerical simulation study, J. Fluid Mech., 518:231-259.

[7] Masri, A., Bilger, R.W., Dibble, R.W., (1990), The local structure of turbulent nonpremixed flames near extinction, Combust. Flame 81:260-276.

[8] Hawkes, E.R., Sankaran, R., Sutherland, J.C., Chen, J.H., (2006), Terascale Direct Numerical Simulations of turbulent nonpremixed CO/H_2 plane jet flames, 11th SIAM International Conference on Numerical Combustion, Granada, Spain, Apr. 23-26.

[9] Marble, M.B., and Broadwell, J.E., (1977), The coherent flame model on non-premixed turbulent combustion. Project Squid TRW-9-PU, Purdue University.

[10] Pope, S.B., (1988), The evolution of surfaces in turbulence, Int. Jnl. Engng. Sci. 26(5):445-469.

[11] Pantano, C., (2004), Direct Simulation of Non-premixed Flame Extinction in a Methane-Air Jet with Reduced Chemistry, J. Fluid Mech. 514: 231-70.

[12] Kennedy, C.A., Carpenter, M.H., (1994), Several New Numerical Methods for Compressible Shear-Layer Simulations, Appl. Num. Math. 14:397-433.

[13] Bilger, R.W., (1976), Combust. Sci. Technol. 13:155-170

[14] Reutsch, G.R., Vervisch, L., Liñan, A., (1995), Effects of heat release on triple flames, Phys. Fluids 7(6):1447-1454.

[15] Daou, J., and Liñan, A. (1998), The role of unequal diffusivities in ignition and extinction fronts in strained mixing layers, Combust. Theory Modelling 2:449-477.

[16] Hewson, J.C., Kerstein, A.R., (2002), Local extinction and reignition in nonpremixed turbulent $CO/H_2/N_2$ jet flames, Combust. Sci. and Technol., 174:35-66.